

20.6 A Blocker-Resilient Wideband Receiver with Low-Noise Active Two-Point Cancellation of >0dBm TX Leakage and TX Noise in RX Band for FDD/Co-Existence

Jin Zhou, Peter R. Kinget, Harish Krishnaswamy

Columbia University, New York, NY

The demand for lower cost and form factor and increased re-configurability in wireless systems has driven the investigation of blocker-tolerant software-defined radios [1-4]. While promising, a reduction in system form-factor will result in lower isolation among antennas due to the co-existence of multiple ratios or lower isolation within duplexers for FDD systems due to their reduced size and/or increased re-configurability. Out-of-band (OOB) powerful modulated TX-leakage due to limited antenna/duplexer isolation imposes challenges that are more severe than those posed by continuous-wave (CW) blockers by several orders of magnitude, including cross-modulation, second-order intermodulation and TX noise in the RX band (Fig. 20.6.1). Analysis shows that in the face of 0dBm peak TX leakage and a -30dBm CW in-band jammer, to achieve -90dBm sensitivity with 7dB SNR over 2MHz signal BW, a transceiver must exhibit +30dBm receiver OOB IIP3 and -160dBc/Hz TX noise in RX band.

In highly-linear current-mode receivers, the OOB linearity is dominated by the LNTA input. TX-leakage cancellation at the receiver input may be pursued using passive and active circuitry. Passive TX leakage cancellation requires bulky LC-based isolation structures that are not amenable to silicon integration and wideband/tunable operation. Active leakage cancellation at the receiver input suffers from NF degradation due to the noise of the cancellation circuitry. Here, we demonstrate a two-point low-noise active TX leakage-cancellation scheme that can (i) cancel up to +2dBm peak TX leakage at the receiver input (30dB higher than prior art [6-7]), enabling a triple beat at +2dBm peak TX leakage (TB_{2dBm}) of 68dB and an effective IIP3 of +33dBm (enhancements of 38dB and 19dB respectively) with an associated increase in receiver NF of <0.8dB, and (ii) effectively suppress TX noise in the RX band by up to 13dB, enabling transmitters with -148dBc/Hz RX-band noise to meet the -160dBc/Hz requirement. This is achieved by (i) embedding the leakage cancellation within a noise-cancelling LNTA so that the noise and distortion of the cancellation circuitry are cancelled, and (ii) performing a second-point cancellation of TX noise in the RX band after the LNTA so that the noise impact is reduced. This enables FDD/co-existence with as low as 25dB TX-RX isolation.

The proposed receiver (Fig. 20.6.1) uses a current-mode architecture with a common-gate (CG) common-source (CS) noise-cancelling LNTA (NC-LNTA) followed by current-driven passive mixers, baseband TIAs, and recombination circuitry. Leakage cancellation is pursued *right at the RX input by repurposing the CG device as a leakage canceller*. A TX signal replica coupled from the TX output is injected at the gate of the CG device of the LNTA with appropriate amplitude and phase scaling, creating a current that cancels the TX leakage at the RX input. This eliminates linearity (cross-modulation) issues in the CS device. *The advantage of this approach is that the noise of the cancellation path, namely the CG device, variable-gain amplifier and phase shifter, is completely cancelled through the noise-cancelling operation of the topology*. While the CS device is protected, the CG device still experiences a large TX-leakage (because of gate injection) and an incident CW jammer, and will generate cross-modulation products. *Interestingly, these products also get cancelled upon recombination through the distortion-cancelling property of the noise-cancelling architecture* [5] – the cross-modulation products are downconverted to baseband in the CG path, but also create a voltage at the RX input that is sensed and amplified by the CS path. Note that an equivalent TX leakage current does flow down the CG path to baseband as a result of the injection, but gets filtered out in the baseband TIA and will not create linearity issues due to the current-mode design. Thus, *cross-modulation challenges are mitigated with ideally no addition of noise*. The leakage current flowing down the CG path can degrade SNR due to TX noise in the RX band. So, a second injection of a TX replica signal is performed in the current domain in the CS path at the LNTA output. With appropriate scaling, TX noise in the RX band can be cancelled when the CS and CG paths are recombined. In general, two-point cancellation is needed as the transfer functions of the TX leakage and TX noise in the RX band through the duplexer/antenna pair will differ. Noise impact of the CS-path injection circuitry is reduced by the LNTA's CS path gain.

Figure 20.6.2 shows the detailed schematic of the receiver. A complementary structure is adopted for the NC-LNTA for high linearity. Thick-oxide transistors

are used for the CG devices of the LNTA to enable cancellation of >0dBm peak TX leakage. The low-resistance current-driven passive mixers are ac-coupled to the LNTA and are driven by an integrated 4-phase 25%-duty-cycle LO generator. The baseband TIAs adopt a Rauch topology [3] for handling large TX leakage. Recombination circuits based on 5-b digitally-controlled binary-weighted differential g_m cells combine I/Q TIA outputs from the CG and CS paths, allowing adjustment of both amplitude and phase from each path. The cancellation path at the gate of the CG device consists of a 5-b digitally-controlled current-mode Cartesian variable-gain phase rotator (PR) and a variable-gain thick-oxide RF TIA buffer. The unit cell of the phase rotator uses a self-biased inverter-like complementary amplifier topology for high linearity. The RF TIA buffer provides low impedance at the output of the PR for wide bandwidth and at the input of the CG device of the LNTA. A scaled version of the 5-b variable-gain PR is used in current-mode in the second CS cancellation path without the RF TIA. The power consumption of the cancellation paths is scalable (13 to 72mW) based on the TX leakage level.

The prototype 65nm CMOS receiver (Fig. 20.6.7) operates over 0.3GHz to 1.7GHz, with peak gain setting of 34dB and widely programmable gain and baseband bandwidth. The measured NF ranges from 4.2dB to 5.6dB (with cancellation circuitry disabled), the out-of-band IIP3 is +12dBm and the input-referred out-of-band blocker power for 1dB compression is +2dBm (Fig. 20.6.3). The use of 8-phase mixing (not pursued here) would lower the NF even further and provide harmonic rejection. TX leakage cancellation experiments are performed using an attenuator to model the finite isolation as well as using a PCB-based planar antenna pair to model a co-existence environment (Fig. 20.6.4) with a transmitter featuring an off-the-shelf +30dBm power amplifier. Using the CG canceller, >30dB suppression at the input is measured across leakage levels and is not limited by isolation group delay. Figure 20.6.4 also shows the triple beat at the receiver output in the presence of an additional in-band -30dBm jammer for varying leakage levels and the equivalent IIP3 that results with and without cancellation. In the absence of cancellation (reducing our receiver to a generic highly-linear receiver with +12 to 14dBm out-of-band IIP3), the TB degrades to 30dB at +2dBm peak TX leakage. However, with the TX-leakage cancellation, 68dB TB_{2dBm} is measured (38dB improvement) enabling an effective IIP3 of +33dBm (19dB improvement). The receiver NF is measured with the CG canceller enabled using the same recombination settings that optimize TB, and the noise-figure degradation is <0.8dB thanks to noise cancellation. With noise cancellation disabled, the NF degrades to 12dB. Cancellation of TX noise in the RX band is also demonstrated (Fig. 20.6.5) for a constant -6dBm peak TX leakage level while varying the relative RX-band noise level (in dBc/Hz). Even though the CS canceller adds noise, the overall receiver noise still gets reduced significantly due to the TX noise cancellation. Up to 13dB effective suppression of TX noise in the RX band is measured. The receiver including the LO divider consumes 75mW-to-83mW power. When compared with the state of the art (Fig. 20.6.6), our work demonstrates the highest modulated leakage handling (TB_{2dBm} and equivalent IIP3), and is the only one that alleviates the TX's RX-band noise requirement.

Acknowledgment:

This work was sponsored by the DARPA RF-FPGA program.

References:

- [1] D. Mahrof et al, "A Receiver with In-Band IIP3>20dBm, Exploiting Cancelling of OpAmp Finite-Gain-Induced Distortion via Negative Conductance," *IEEE RFIC Symp.*, pp. 85-88, June 2013.
- [2] D. Murphy et al, "A Blocker-Tolerant Wideband Noise-Cancelling Receiver with a 2dB Noise Figure," *ISSCC Dig. Tech. Papers*, pp. 74-75, Feb. 2012.
- [3] I. Fabiano et al, "SAW-Less Analog Front-End Receivers for TDD and FDD", *ISSCC Dig. Tech. Papers*, pp. 82-83, Feb. 2013.
- [4] C. Andrews et al, "A Passive Mixer-First Receiver with Digitally Controlled and Widely Tunable RF Interface," *IEEE J. Solid-State Circuits*, vol. 45, no. 12, pp. 2696-2708, Dec. 2010.
- [5] S. Blaakmeer et al, "Wideband Balun-LNA With Simultaneous Output Balancing, Noise-Canceling and Distortion-Canceling," *IEEE J. Solid-State Circuits*, vol. 43, no. 6, pp. 1341-1350, June 2011.
- [6] H. Khatri et al, "An Active Transmitter Leakage Suppression Technique for CMOS SAW-Less CDMA Receivers," *IEEE J. Solid-State Circuits*, vol. 45, no. 8, pp. 1590-1601, Aug. 2010.
- [7] V. Aparin et al, "An Integrated LMS Adaptive Filter of TX Leakage for CDMA Receiver Front-Ends," *IEEE J. Solid-State Circuits*, vol. 41, no. 5, pp. 1171-1182, May 2006.

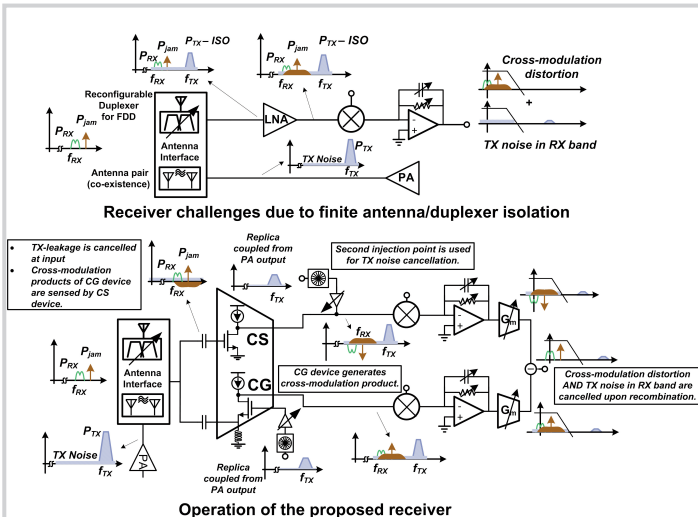


Figure 20.6.1: Challenges posed by modulated TX leakage and suppression of these mechanisms in our proposed receiver.

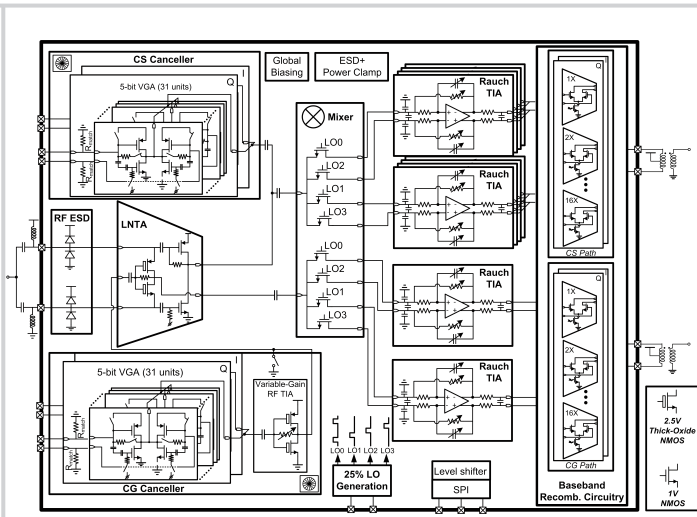


Figure 20.6.2: Proposed receiver with low-noise active two-point cancellation of TX leakage and RX-band noise.

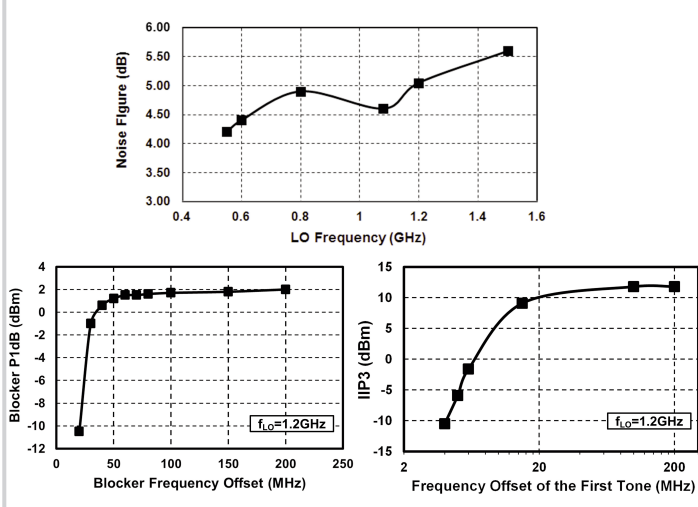


Figure 20.6.3: Measured NF (cancellation circuits inactive), input-referred blocker power for 1dB compression, and IIP3.

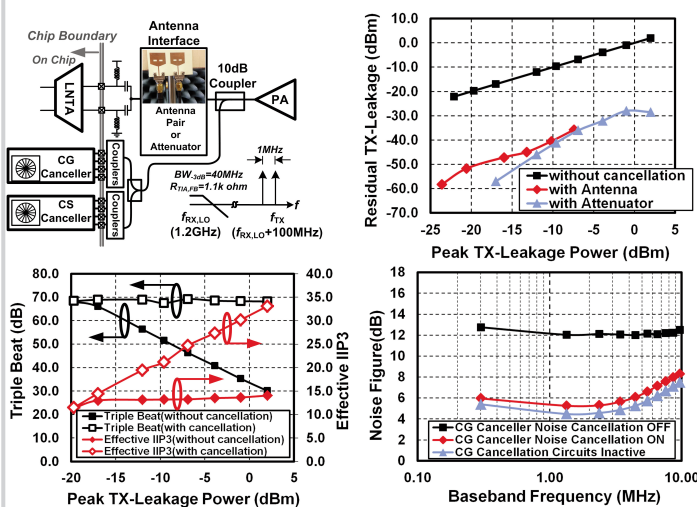


Figure 20.6.4: TX leakage, TB, effective IIP3, and NF with/without CG-path leakage cancellation.

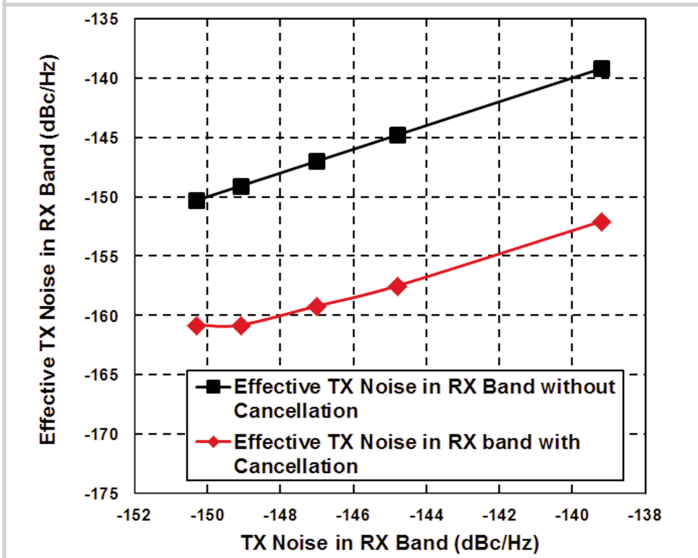


Figure 20.6.5: Measured TX noise in the RX band.

| Architecture | TX Leakage Cancellation/Suppression | | Highly-Linear Software-Defined Radio | | This work |
|--|---|--|--------------------------------------|--|----------------------------------|
| | Active TX Leakage Suppression After LNA | Active TX Leakage Cancellation After LNA | High Linearity Passive Mixer-First | Mixer First with Distortion Cancellation | |
| CMOS Technology | 180nm | 250nm | 65nm | 65nm | 65nm |
| RF Frequency | 1.96GHz | 800MHz | 0.1-2.4GHz | 0.2-2.6GHz | 1.8-2.4(TDD)/1.8-2.1(FDD) GHz |
| Gain | 45dB | 14.8dB (LNA) | 40-70dB | 26.5dB | 45.5dB |
| Baseband BW | N/A | N/A | 20MHz ² | 12MHz | 1.4(TDD)/3.4(FDD) MHz |
| DSB NF | 3.1dB | 1.4dB (LNA) | 4dB | 7.5dB | 3.8(TDD)/3.1(FDD) dB |
| Blocker P1dB | N/A | N/A | +4dBm ² | N/A | N/A |
| Out-of-band IIP3 | N/A | N/A | +25dBm | +10/+18dBm ⁴ | +18(TDD)/+16(FDD) dBm |
| Maximum Handled Peak TX Leakage | -28dBm ⁵ | -28dBm ⁷ | N/A | N/A | N/A |
| NF Degradation due to Leakage Cancellation | 1.8dB | 1.3dB (LNA) | N/A | N/A | N/A |
| TB _{2dBm} ⁶ | 9dB ⁹ | N/A | 52dB ¹⁰ | 22/38dB ¹⁰ | 38(TDD)/34(FDD) dB ¹⁰ |
| TX Noise Cancellation | N/A | N/A | N/A | N/A | N/A |
| RX Power Consumption | 114mW | N/A | 37-70mW | 17.3-36.7mW | 30.7mW |
| Canceller Power Consumption | 48mW | 43mW | N/A | N/A | N/A |
| Active Area | N/A | N/A | 2mm ² | 0.2 mm ² | 0.74 mm ² |

Figure 20.6.6: Measurement summary and comparison table.

¹ Maximum BW ² Blocker at 40MHz offset ³ Blocker at >60MHz offset ⁴ First tone at 135MHz > 450MHz offset
⁵ Effective IIP3 for TX leakage under cancellation of +2dBm peak TX leakage ⁶ 3dB Peak-to-average ratio
⁷ 6dB Peak-to-average ratio ⁸ Triple beat at +2dBm peak TX leakage power ⁹ Calculated from reported TB at -28dBm TX leakage level
¹⁰ Calculated from reported IIP3 (IIP3=0.5*TB+P_{TX,avg}[6]) *Metrics related to the TX leakage cancellation are highlighted with*

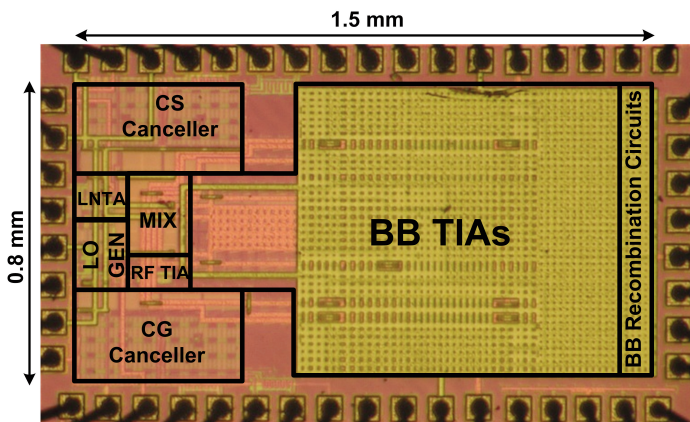


Figure 20.6.7: Die micrograph.